Global Optimization of H-Passivated Si Clusters with a Genetic Algorithm

Yingbin Ge and John D. Head*

Department of Chemistry, University of Hawaii, 2545 The Mall, Honolulu, Hawaii 96822

Received: January 11, 2002; In Final Form: April 23, 2002

We have developed a genetic algorithm (GA) for the global geometry optimization of fully and partially H-passivated Si clusters. Since it is not obvious how many H atoms will bind to a Si cluster, one important feature of our GA is that it can automatically select between different amounts of H passivation. The GA uses the AM1 semiempirical method for the fast calculation of individual locally optimized geometries for use in the GA evolution process. Although the AM1 method produces reasonable Si_xH_y optimized geometries, we perform a more accurate energy ranking of the low energy structures generated by the GA with B3LYP density functional theory and MP2 calculations. We use the GA to determine the low energy structures for the clusters $Si_{10}H_m$, with $m = 4, 8, 12, 16, 20$, and $Si_{14}H_{20}$. The Si_{10} framework evolves from compact structures to more open structures with increasing numbers of H atoms and we find Si_{10} is essentially fully passivated with 16 H atoms. Adding H atoms causes substantial changes in the Si_{10} framework once all the Si atoms are four coordinate. We also find the Si framework in the global geometry of the fully H passivated clusters such as $Si_{10}H_{16}$ and $Si_{14}H_{20}$ to adopt the structure of a bulk Si lattice fragment providing B3LYP and MP2 energy calculations are performed.

Introduction

Silicon nanoparticles have attracted a lot of interest because of their potential use as material for fabricating electronic and electroptical devices. A number of theoretical and experimental studies have investigated the stable geometries for small and medium sized Si only clusters.[1−12] Some type of surface passivated particle will be needed if Si nanoclusters are to be used in a robust commercial device. In this paper we theoretically investigate the stable geometries formed by H-passivated Si clusters. While it seems most likely for a completely passivated nanocluster that the atoms in the underlying Si cluster should form a diamond lattice-like arrangement, it is not obvious how many H atoms are required to completely passivate a Si cluster or indeed whether the diamond like structure for a Si framework actually does correspond to the most stable geometry. Estimation of the number of H atoms binding to a Si cluster is further complicated when the possibility of structures containing rings of Si atoms or the formation of relatively unstable Si-Si multiple bonds is considered. Even a medium-sized cluster can have a huge number of stable local geometries and an exhaustive search for the global structure minimum is extremely hard to perform. Several groups have theoretically explored some of the possible structures for small[13] to medium sized[14−17] silicon hydride clusters. We report here a genetic algorithm (GA) we have developed as a strategy to find the global energy minimum corresponding to the most stable structure for various Si_xH_y clusters. The GA is a global optimization strategy inspired by the Darwinian evolution process. Since 1990, GAs have been widely used to search for the global minimum of atomic clusters and molecular agglomerates.[12,18−22] Some of the previous workers have used simulated annealing methods coupled with either plane wave DFT[14,15] or semiempirical MINDO/3 [16] calculations as an alternative global optimization strategy for

the silicon hydride clusters. We choose the GA approach because it can also identify many of the low energy cluster structures while seeking the global minimum. Furthermore, the stochastic nature of the GA is temperature independent and avoids the problem of a geometry getting trapped into a specific local minimum which can occur with simulated annealing as the molecular system is cooling.[23]

The GA explores a large number of different cluster conformations and consequentially requires a computational method which can evaluate the total energy of specific cluster geometry rapidly. Ho and co-workers obtained energy values via a TB-DFT method in their implementation of a GA to find the structures of medium-sized silicon clusters.[12] Presently these TB-DFT methods are only parametrized for use with a single element. Due to the binary nature of the Si_xH_y clusters we perform our energy evaluations with the semiempirical AM1 method.[24] Once the GA selects a specific cluster conformation the AM1 energy calculations are relatively fast enabling a rapid gradient based optimization to the nearest local minimum. The AM1 energy has the important feature of a solid quantum mechanical basis so that no additional empirical information is required to identify which atom pairs in the cluster combine to form bonds. Thus a H atom in a Si_xH_y cluster has the option of forming a bond with either a Si atom or another H atom depending on which bond gives the lower cluster total energy. As a consequence, when a Si cluster is completely H-passivated, any remaining excess H atoms can pair up to form hydrogen molecules.

Simulated annealing optimization also involves a large number of energy function evaluations and Meleshko et al. selected the semiempirical MINDO/3 method for their procedure.[16] The computer times needed for either MINDO/3 or AM1 calculations are comparable, but experience by us and others[25,26] suggest that AM1 is presently the semiempirical method which gives the most reliable optimum geometries and relative total energies for Si containing compounds. However, since we obtain

* To whom correspondence should be addressed. Phone: 808-956-5787. Fax: 808-956-5908. E-mail: johnh@hawaii.edu.

several different geometries close in AM1 energy in a GA run on a specific Si_xH_y cluster, we also examine the relative energy ordering of a small subset of the low AM1 energy structures by performing ab initio second-order Møller−Plesset (MP2) and density-functional theory with the B3LYP functional (B3LYP) calculations using the optimized AM1 geometries as starting structures.

In the next section we describe in more detail the GA and the methods used for evaluating the cluster total energy. In the third section we first present results for application of the GA to a series of $Si_{10}H_m$ clusters and show how the cluster geometry evolves as the Si_{10} cluster becomes completely passivated with H. We then discuss the efficiency of the GA. In the final part of the results section we describe the global optimization of $Si_{14}H_{20}$ and the formation of a diamond lattice structure for the Si atoms. Concluding remarks are given in the final section of the paper.

Computational Method

To find the more stable isomers for a Si_xH_y cluster requires a large number of total energies at different cluster geometries to be evaluated. Standard AM1 semiempirical energy calculations[24] are used in the GA to facilitate a computationally fast comparison of the relative stability of various optimized Si_xH_y geometries. We define the cluster binding energy BE_i for the ith structure as

$$BE_i = E_{Si_xH_y} - xE_{Si} - yE_H \quad (1)$$

where $E_{Si_xH_y}$ is the total energy of the optimized cluster geometry and E_{Si} and E_H are the ^3P and ^2S ground-state energies of the Si and H atoms, respectively.

Although AM1 is time-efficient for the GA, it could not be relied on to accurately order the stability of different cluster isomers close in energy. Hence, we pick up the best several structures found by our GA, and then further optimize them by ab initio second-order Møller−Plesset (MP2)[27] and density-functional theory using the B3LYP functional (B3LYP)[28] calculations. As suggested by Raghavachari and Rohfling[29] the MP2 and B3LYP geometry optimizations were performed using the Hay−Wadt effective core potential (ECP) and valence basis set for Si[30] augmented with a d function[29] and the Dunning-Hay basis for H.[31] The AM1 and MP2 calculations were performed using the GAMESS program,[32] and the B3LYP calculations were performed with Gaussian 94.[33] Raghavachari and Rohfling show the HW-ECP and basis set at the MP4 level does an excellent job of reproducing the results obtained with all electron calculations on Si only clusters.[30] In the present work we find calculations at the MP2 and MP4 levels to give essentially the same energy order for the $Si_{10}H_4$ and $Si_{10}H_{16}$ series of clusters: where some energy reordering does occur for some of the high energy $Si_{10}H_{16}$ structures which are within 2 kcal/mol of each of other. Krüger and Sax have recently found the 6-31G** B3LYP functional, as well as other functionals, to give reasonable geometries and relative energies for different isomers of Si_2H_2 and Si_2H_4.[34] We find the HW-ECP and basis with the B3LYP functional to reproduce the Krügger and Sax calculations. As a consistency check on the ab initio calculations, we report the results of both B3LYP and MP2 calculations instead of performing the much more computationally demanding MP4 calculations. A complete tabulation of the final cluster geometries and relative energies are available from the authors.

The GA works by randomly selecting and mating the more fit individuals in a generation to produce next generation of offspring, where the fitness is a measure of the energetic stability for an individual optimized cluster geometry. The GA selects new cluster conformations which are likely to have lower optimized energies than structures in previous generations. The population size of the GA is set to N, which is the total number of Si and H atoms in the cluster to be globally optimized. Our experience finds that a variable N is needed to prevent premature GA convergence for the larger clusters and to avoid low convergence efficiency for the smaller clusters. We generate N initial structures of the H-passivated Si clusters by first putting the Si atoms into a cubic box randomly, and then we randomly arrange H atoms outside the box. That is, we generate initial structures with the assumption that the stable structures of the H-passivated Si cluster will tend to have H atoms on the surface instead of inside. However, to reduce this bias, we also allow a small number of H atoms inside the box nearby the borderline. Then we optimize the geometry of the above N structures by the AM1 method to create our ancestor population. The fitness f_i of the ith initial individual cluster is based on a Boltzman distribution:

$$f_i = \exp\left(\frac{C - BE_i}{NRT}\right) \quad (2)$$

where BE_i is the optimized AM1 cluster binding energy, and C is a constant, whose value is set to be the lowest energy obtained from the initial N ancestors. C is used to rescale the fitness f_i into a rather small range. The value of C will not affect the probability of one parent being selected. RT is set to 0.2 eV/atom, which corresponds to a temperature of 2300 K. Roulette selection is used to select N random parent couples for the next generation. The probability P_i of the ith geometry being selected is determined by the normalized fitness of that cluster:

$$P_i = f_i / \sum_i^{f_i} \quad (3)$$

The same individual cluster geometry can be selected more than once during the roulette selection. Each resulting parent is then randomly rotated about their center of mass. From previous work on atomic clusters we adopt three possible mating methods. One approach is to take the arithmetic mean of the Cartesian coordinates from two parent geometries.[18,20] The second method is to take a fragment of Si atoms from one parent and replace it with the fragment of the other parent with the same number of atoms, and also cut a fragment of H atoms from one parent and replace it with a fragment of H atoms in the other parent with the same number of atoms.[18,20] The last method is to cut each parent into halves and then recombine one-half from each parent to generate the offspring.[22] The first and second mating processes produce drastic mutations, while the third method retains much of the local structures of both parents.[22] The probabilities used for selecting the first, second and third methods are 25%, 25%, and 50%, respectively. After the mating process, N offspring are generated and fully optimized again by the AM1 method. We replace the least stable structure of its parent population with a new offspring if it has relatively lower energy. A number of different convergence strategies have been proposed.[20,21] To enable an equal treatment on the different sized clusters we found it best to take the GA as being converged when the lowest energy structure remains the same for the last $3N$ continuous generations. The final structures we tabulate correspond to the lowest optimized energies found during an entire GA run.

Global Optimization of Si Clusters

J. Phys. Chem. B, Vol. 106, No. 28, 2002 **6999**
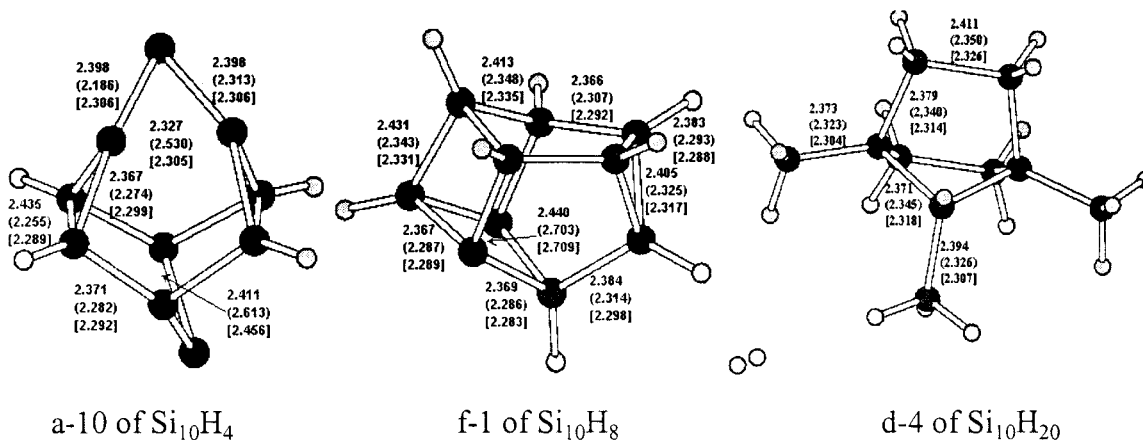
Figure 1. Representative optimized cluster structures obtained with the AM1, B3LYP and MP2 methods. The structures are (a) $Si_{10}H_4$ a-10, (b) $Si_{10}H_8$ f-1, and (c) $Si_{10}H_{20}$ d-10(5) dissociated into $Si_{10}H_{18}$ and a H_2 molecule. The three bond lengths are listed in the order AM1, (B3LYP), and [MP2] in angstroms.

Results and Discussion

We start this section by examining the effectiveness of the GA at identifying chemically reasonable low energy structures of Si clusters. We applied the GA to a series of $Si_{10}H_m$ clusters, with $m = 4, 8, 12, 16$ and 20. Clearly the Si framework will only be partially passivated by H when m is small, but it is less clear how many H atoms are needed to ensure all the Si atoms in a cluster are tetrahedrally coordinated and fully saturated with four bonds. The determination of the number of H atoms needed is further complicated by the Si atoms in the cluster being able to form ring structures or perhaps even Si=Si double bonds. One goal of the present work is not just to develop a method which finds the most stable structures of binary clusters with specific stoichiometries, but also to show that our GA approach can determine how many H atoms are preferred in a cluster. Following the discussion of the $Si_{10}H_m$ results and the effectiveness of the GA for investigating passivation of Si clusters, we extend our calculations to the $Si_{14}H_{20}$ cluster. The Si framework in $Si_{14}H_{20}$ can be arranged as a diamond lattice-like fragment, where this fragment has 20 Si dangling bonds which can be saturated with the 20 H atoms. We apply the GA to $Si_{14}H_{20}$ to determine whether the diamond like structure is the most stable structure for this cluster.

The key structural results for the series of $Si_{10}H_m$ clusters are presented in Figures 1–6. Since we do obtain different relative stabilities by the semiempirical and nonempirical calculations each structure in the figures is labeled by c–X where c is an alphabetical character ordering the AM1 structures by decreasing binding energy and X is a number indicating the relative binding energy as calculated by the B3LYP functional. Generally we found the binding energy order calculated by MP2 follows the B3LYP ordering, but in the cases where they do differ we add the MP2 order in parentheses to the c–X structure label. Thus structure d-9(7) of $Si_{10}H_4$ in Figure 2 is the fourth AM1, ninth B3LYP, and seventh MP2 lowest energy structure. The figures show the B3LYP optimized geometries obtained by starting with coordinates from the AM1 optimized structure produced by the GA. Despite the problems with the relative energy ordering, the geometries obtained with the AM1, MP2 and B3LYP for a particular structure all exhibit the same general features. To illustrate the degree of typical similarity we show in Figure 1 AM1, MP2, and B3LYP structures obtained for the a-10 $Si_{10}H_4$, f-1 $Si_{10}H_8$, and d-11 $Si_{10}H_{20}$ clusters. It is worth noting that the lines connecting pairs of Si atoms are drawn by the graphics program only when the two atoms are within 2.45
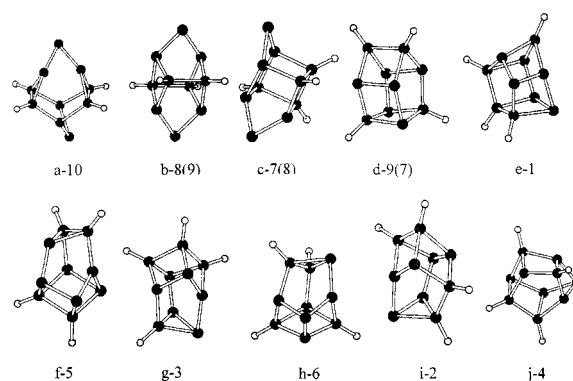
Figure 2. Ten lowest AM1 energy structures for $Si_{10}H_4$. The numbers label the B3LYP and MP2 energy rankings as explained in the text.

Å of each other and a line only approximately indicates that a bond is actually formed between a pair of atoms. Below we present in more detail the different structural features found for the various $Si_{10}H_m$ clusters in turn.

$Si_{10}H_4$. Figure 2 shows the 10 structures with lowest AM1 energy obtained by the GA for $Si_{10}H_4$ and their rankings with the B3LYP and MP2 methods. The $Si_{10}H_4$ cluster attempts to form compact structures presumably so as to reduce the number of Si atoms not tetrahedrally coordinated. Each H atom binds to a different Si atom and each of these hydrogenated Si atoms are tetrahedrally coordinated with 3 additional neighboring Si atoms. The 3 most stable AM1 structures a-10, b-8(9), and c-7(8) differ in energy by less than 0.5 kcal/mol. Structures a-10, b-8(9), and c-7(8) are the only structures we find that contain two Si atoms which are only doubly coordinated. The MP2 and B3LYP calculations show these structures to be the least stable of those shown in Figure 2. The Si parameters used by the AM1 method were obtained from a set compounds where the Si atom is generally coordinated by four other atoms,[35] and the AM1 parameters most likely are not optimally designed to reliably treat low coordinate Si atoms. The present calculations suggest that AM1 overestimates the stability of a biradical localized on on the 2 coordinate Si atoms. Figure 1 shows the AM1, B3LYP, and MP2 methods produce the same basic optimized a-10 geometry, even though B3LYP and MP2 compute a-10 to be 56.2 and 82.3 kcal/mol, respectively, higher in energy than the e-1 structure. Structure e-1 is the most stable structure calculated by B3LYP and MP2. Energetically structures e-1–j-4 differ by 3.4 kcal/mol in the AM1 calculations, while the B3LYP and MP2 calculations produce differences of 24.6 and 28.6 kcal/
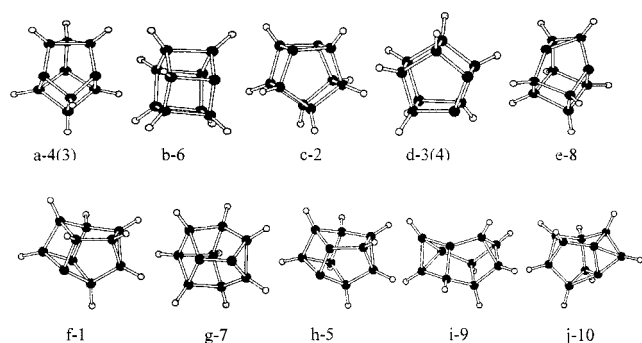
a-4(3)   b-6   c-2   d-3(4)   e-8

f-1   g-7   h-5   i-9   j-10

Figure 3. Ten lowest AM1 energy structures for $Si_{10}H_8$.

a-2   b-1   c-3(4)   d-4(3)   e-9(8)

f-5   g-8(9)   h-6   i-7   j-10

Figure 4. Ten lowest AM1 energy structures for $Si_{10}H_{12}$.

mol, respectively. Geometrically structures e-1 and j-4 have a similar Si_{10} skeleton made up of 5 Si_4 rings but with different H atom arrangements. A second type of Si_{10} framework containing one Si_3 ring is found for the i-2, g-3, f-5, and h-6 structures. Presumably the Si_3 ring is more strained than the larger rings causing the i-2 structure to be 4.0 (B3LYP) and 3.8 (MP2) kcal/mol less stable than e-1. The three-membered rings in i-2 and g-3 have one of the Si atoms H passivated, whereas f-5 and h-6 have two of the Si atoms H passivated further enhancing the Si_3 ring strain. Even though j-4 does not contain any three-membered Si rings, it maybe less stable than e-1 because two of the three coordinate Si atoms bind to three H-passivated Si atoms thereby producing 2 isolated dangling bonds; in all the other structures every three-coordinate Si atom is adjacent to at least another three-coordinate Si atom.

$Si_{10}H_8$. Figure 3 shows the 10 most stable structures obtained for the $Si_{10}H_8$ cluster using the AM1 energy and the GA. The four extra H atoms continue to complete the tetrahedral coordination favored by Si and in a number of structures the Si skeleton from $Si_{10}H_4$ is retained. For example, structures b-6, c-2, and d-3(4) in Figure 3 have the same Si_{10} framework as for e-1 of $Si_{10}H_4$, while the $Si_{10}H_8$ structures f-1, a-4(3), h-5, g-7, and e-8 have the same Si skeleton found for $Si_{10}H_4$ i-2 structure. In all of the $Si_{10}H_8$ structures, Si only binds to one H atom and Figure 3 suggests the two remaining unpassivated Si atoms are always 3 coordinate. The AM1 energy variation for the different $Si_{10}H_8$ structures is much larger than found for $Si_{10}H_4$ and ranges over 8.6 kcal/mol for structures a-4(3) to f-1. At the B3LYP and MP2 levels we find f-1 to be the most stable structure. We think this structure is favored because the two unpassivated Si atoms can get within 2.7 Å of each other along the four membered ring diagonal and form a weak Si–Si bond. A comparison of the AM1, B3LYP and MP2 structures for f-1 are given in Figure 1. The bond lengths predicted by the B3LYP and MP2 methods are very similar with a deviation of less than 0.02 Å, while the AM1 distances are within 0.1 Å of the ab initio values. A comparison of the f-1 structure with the $Si_{10}H_4$ a-10 structure shows the Si–Si bond lengths of $Si_{10}H_8$ are longer due to more H passivation, and they are closer to the experimental 2.3517 Å Si–Si distance in a diamond lattice structure.[36] F-1 is 2.5 (B3LYP) and 5.3 (MP2) kcal/mol more stable than c-2, and both structures have the 2 unpassivated Si diagonally opposite each other in a four membered ring. However, in contrast to what was found for $Si_{10}H_4$, f-1 appears to be stabilized by a three membered ring of Si–H atoms relative to c-2. The next higher energy structures a-4(3) and d-3(4) resemble f-1 and c-2, respectively, but with the unpassivated Si atoms at different locations. The MP2 energy favors the three-member ring and has a-4(3) 1.6 kcal/mol more stable than d-3(4) whereas B3LYP gives 2.6 kcal/mol for the reverse stability.
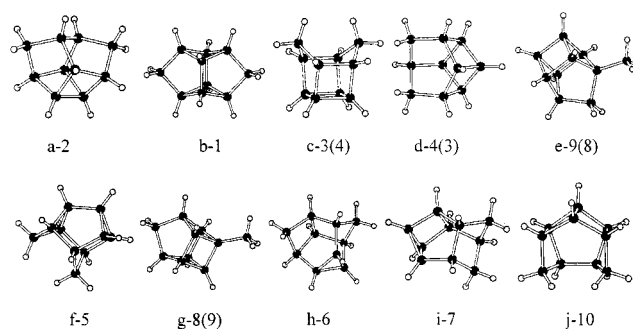
$Si_{10}H_{12}$. There are now enough H atoms in the $Si_{10}H_{12}$ clusters shown in Figure 4 to ensure all of the Si atoms are four coordinate. Figure 4 also shows all of the structures to have five rings of Si atoms: this number of rings must be formed if each of the Si atoms is four coordinate and no multiple Si–Si bonds are formed. Typically eight of the Si atoms bind with a single H atom and the two remaining Si atoms form SiH_2; although in the higher energy structures g-8(9) and e-9(8) a SiH_3 group is formed and one Si atom is tetrahedrally coordinated by 4 other Si atoms. Presumably because the Si coordination is now complete the low energy structures obtained by AM1 match better with the B3LYP and MP2 energy ordering. The two lowest energy structures b-1 and a-2 appear to have a Si framework quite different to those previously found for the $Si_{10}H_4$ and $Si_{10}H_8$ clusters and they differ in energy by 2.7, 1.3 and 0.7 kcal/mol at the AM1, MP2 and B3LYP levels, respectively. The next structure c-3(4) is 1.4 (AM1), 7.4 (B3LYP), and 10.2 (MP2) kcal/mol above the second lowest energy structures and has a Si skeleton easily derived by adding H atoms to structures c-2 or d-3 found for $Si_{10}H_8$. Structure d-4(3) is only 2.5 (AM1), 0.8 (B3LYP) and −0.03 kcal/mol (MP2) above c-3(4) and corresponds to an opening of the Si_3 ring of the $Si_{10}H_8$ f-1 structure. New Si_{10} skeletons are also found for the f-5, h-6 and i-7 structures. Structures e-9(8) and g-8(9) have the same Si_9 framework but place the SiH_3 group at different positions and have their largest energy difference of 0.8 kcal/mol at the AM1 level. We also find the numbers of smaller three- and four-member Si rings in Figure 4 are less than those of in the less H-passivated Si clusters suggesting there is now less strain on the Si_{10} framework.

$Si_{10}H_{16}$. In Figure 5 we show the 20 $Si_{10}H_{16}$ structures corresponding to the 20 lowest AM1 optimized energies we obtain with the GA. Since the j-1 structure had the lowest B3LYP and MP2 energy among the first 10 AM1 structures we display 10 additional structures so as to ensure that other low energy structures, such as m-2(4), are not overlooked. The H atoms in the $Si_{10}H_{16}$ clusters continue to aid forming four coordinate Si atoms. Consistent with the formation of 4 new Si–H bond, each of the Si frameworks in Figure 5, apart from c-19 and l-20, now contain only three rings of Si atoms and as a consequence the Si framework is substantially different to that found in $Si_{10}H_{12}$. Unfortunately, the AM1 energy values exhibit a much narrower range of energy variation, all of the structures in Figure 5 are within 5.8 kcal/mol of each other. The structure with lowest B3LYP and MP2 energy, j-1, is particularly interesting because the Si framework adopts a diamond lattice-like arrangement suggesting the H-passivated Si clusters do prefer a diamond like structure for the Si atoms. Structures m-2(4), b-3(2), and a-4(3) are 5.1, 5.5, and 5.7 kcal/mol at the B3LYP level and 4.5, 2.8, and 3.2 kcal/mol at the MP2 level less stable than the j-1 structure. It is also interesting
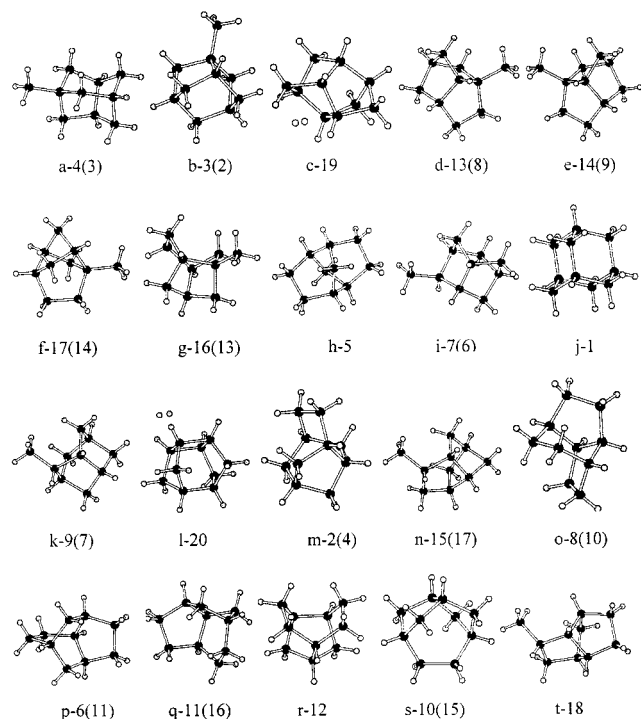
Global Optimization of Si Clusters

J. Phys. Chem. B, Vol. 106, No. 28, 2002 **7001**

Figure 5. Twenty lowest AM1 energy structures for $Si_{10}H_{16}$.

Figure 6. Twenty lowest AM1 energy structures for $Si_{10}H_{20}$.

that the GA manages to find two enantiomers, clusters d and e, which are mirror images of each other.

Figure 5 also contains two structures with 4 rings of Si atoms, c-19 and l-20, which corresponds to a separate $Si_{10}H_{14}$ cluster and H_2 molecule. Thus, the GA is giving the first indication that the Si_{10} framework is starting to become saturated when there are 16 H atoms. Energetically c-19 is computed to be 24.6 (B3LYP) and 15.8 kcal/mol (MP2) less stable than the most stable B3LYP structure j-1. The binding energy expression given by eq 1 effectively becomes for the c-19 and l-20 structures

$$BE_i = E_{Si_{10}H_{14}} + E_{H_2} - 10E_{Si} - 16E_H \qquad (4)$$

Equation 4 suggests that if $Si_{10}H_{14}$ was the preferred passivation product over $Si_{10}H_{16}$ at 0 K, then the magnitude of the BE for c-19 should be larger than for the j-1 structure. That is, our GA strategy automatically identifies whether a lower $Si_{10}H_m$, $m <$ 16, passivated cluster is a more stable structure. The $Si_{10}H_{14}$ cluster shown in Figure 5 for c-19 should represent the lowest energy structure possible for $Si_{10}H_{14}$, although since c-19 and l-20 have the highest B3LYP and MP2 energies in the 20 structures shown we may not be sampling enough of the $Si_{10}H_{14}$ low energy structures to correctly identify the most stable $Si_{10}H_{14}$ cluster. At higher temperatures, the larger combined entropy of $Si_{10}H_{14}$ and H_2 should eventually favor their formation. An estimate for the entropic contribution can be obtained from scaled AM1 frequency calculations.[37] In general, we do not find the preferred passivation product to be significantly altered when we include AM1 zero point energy corrections in eq 4. However, at 298 K we estimate from the vibrational calculations that $Si_{10}H_{14}$ and H_2 will only be preferred when their total BE is less than 6 kcal/mol above the $Si_{10}H_{16}$ BE. Since both the B3LYP and MP2 calculations give a BE for c-19 considerably larger that 6 kcal/mol than the j-1 structure we conclude $Si_{10}H_{16}$ has the preferred passivation.

$Si_{10}H_{20}$. Figure 6 shows the 20 lowest AM1 structures found for $Si_{10}H_{20}$. At the B3LYP and MP2 levels the 4 most stable $Si_{10}H_{20}$ structures given in Figure 6 correspond to different
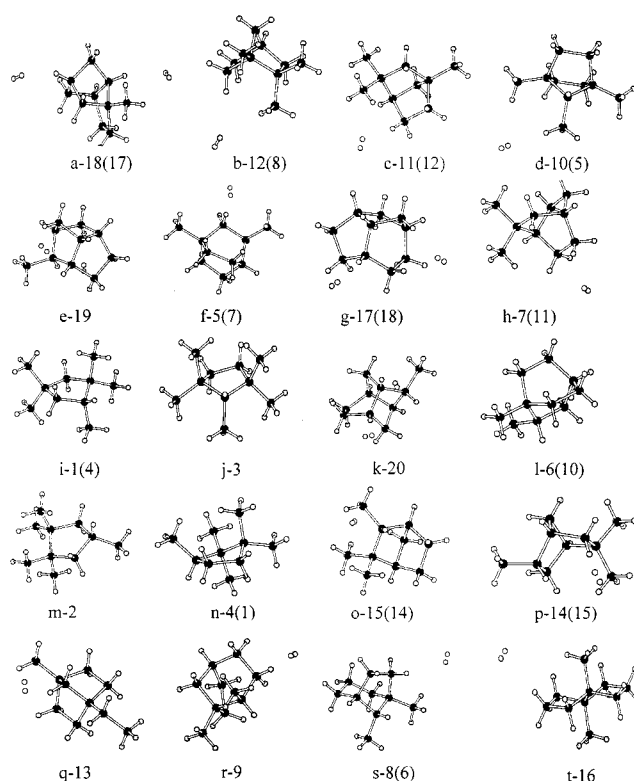
isomers of a tetrasilyl cyclopentasilane. It is difficult to determine which isomer is the most stable since the 4 structures are within 0.8 (B3LYP) and 0.5 (MP2) kcal/mol of each other. The next 12 higher nonempirical energies correspond to structures containing a $Si_{10}H_{18}$ cluster and one H_2 molecule. At the B3LYP level structures f-5(7) and t-16 range from 9.3 to 15.2 kcal/mol above the i-1(4) lowest energy structure, while at the MP2 level d-10(5) through t-16 are only 5.7−9.7 kcal/mol above the n-4(1) structure. For comparison, the AM1 energy varies only 5.3 kcal/mol for all 20 structures. Figure 1 shows the geometry calculated by AM1, B3LYP and MP2 for the d-10-(5) structure in more detail and again confirms the B3LYP and MP2 methods predict very similar geometries, while AM1 exhibits larger geometric differences but preserves the main structural features. From the B3LYP and MP2 energies we can conclude that $Si_{10}H_{20}$ is the more stable passivated structure at 0 K. At 298 K we estimate via AM1 frequency calculations an entropic contribution favoring H_2 loss when the $Si_{10}H_{18}$ and H_2 energies are within 11 kcal/mol of the $Si_{10}H_{20}$ electronic energy. Thus we anticipate a relatively low temperature should cause $Si_{10}H_{20}$ to lose H_2 and produce $Si_{10}H_{18}$.

The four remaining structures g-17(18), a-18(17), e-19 and k-20 in Figure 6 consist of a $Si_{10}H_{16}$ cluster and two H_2 molecules. The energetic cost at 0 K of forming these two hydrogen molecules ranges from 22.2 to 26.7 kcal/mol for B3LYP and 13.2 to 16.5 kcal/mol for MP2 and we can again conclude that the passivation in $Si_{10}H_{16}$ is less favored relative to $Si_{10}H_{20}$. Interestingly, following the same relative AM1 binding energy ordering, the $Si_{10}H_{16}$ structures in a-18(17) and g-17(18) in Figure 6 match with the structures e-14(9) and q-11-(16), respectively, shown in Figure 5. However, the $Si_{10}H_{16}$ clusters shown in the e-19 and k-20 structures in Figure 6 do not match with any of the structures shown in Figure 5. This result demonstrates that the GA in its search for a global minimum does not exhaustively find all of the other low energy structures possible for a particular cluster type. Entropic

7002 *J. Phys. Chem. B, Vol. 106, No. 28, 2002*

Ge and Head
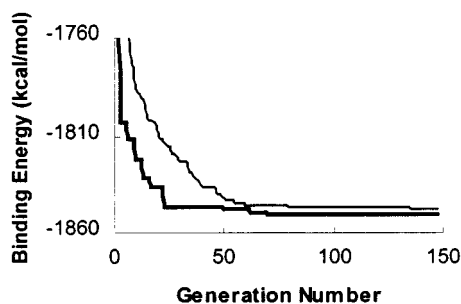
Figure 7. GA evolution for $Si_{10}H_{16}$. The graph shows how the cluster binding energy of the lowest (dark line) and highest (light line) energy individual in each population varies with generation number.

contributions at 298 K, estimated via AM1 frequency calculations stabilize the $Si_{10}H_{16}$ formation by about 20 kcal/mol relative to $Si_{10}H_{20}$ suggesting that $Si_{10}H_{16}$ is the preferred passivation of the Si_{10} cluster at higher temperatures.

$Si_{10}H_m$ Structure Evolution. To summarize, the Si_{10} framework changes from compact cages when only partially passivated by H atoms to more open structures when $m = 12$, 16, and 20 with all the Si atoms becoming four coordinate. Substantial changes in the Si_{10} framework occur between $Si_{10}H_{12}$ and $Si_{10}H_{16}$ because of the Si ring opening which must take place if the structures are to accept additional H atoms. Miyazaki et al. found a similar evolution of compact to open structures in their investigation of Si_6H_m clusters with $0 \leq m \leq 14$.[15] Our GA results also suggest that at 0 K the Si_{10} framework to be fully passivated with 16 H atoms, although we do find that $Si_{10}H_{20}$ can form tetrasilyl cyclopentasilane isomers. The formation of these $Si_{10}H_{20}$ isomers is consistent with the Miyazaki et al. results which find the complete family of Si_6H_m clusters to be stable. Entropic contributions at higher temperatures appear to favor $Si_{10}H_{16}$ as the preferred passivation of the Si_{10} clusters. Unfortunately, the large number of energy evaluations needed by the GA means that it is only practical to estimate the entropic stabilization of differing amounts of H passivation only after identifying possible candidate structures at 0 K.

Effectiveness of the Genetic Algorithm. The above results for the $Si_{10}H_m$ clusters demonstrate the GA to be a useful tool for locating several of the low energy isomers possible for a particular cluster without biasing the calculations toward some preconceived notion of what the most stable structure might be. The GA serves to dramatically reduce the number of energy function evaluations while randomly evaluating many of the more stable isomers of a cluster. To test the consistency of our GA algorithm, we performed two additional GA runs on each specific Si_xH_y cluster using different randomly chosen starting structures. We found all three GA runs to give the same lowest energy structures for the $Si_{10}H_m$ clusters, with $m = 4$, 8, 12, 16, while for the $Si_{10}H_{20}$ and $Si_{14}H_{20}$ slightly different lowest energy structures were produced but all with 3 kcal/mol of each other. In Figure 7 we show the search evolution in one of our typical GA runs on the $Si_{10}H_{16}$ cluster, we find similar evolution patterns for all the other Si cluster described in this paper. The dark line gives the binding energy for the $Si_{10}H_{16}$ structure with lowest energy, the lighter line gives the binding energy for the structure with highest energy in the population, the 26-th structure. In the first 25 generations, the binding energy of the most stable structure drops rapidly to -1846.2 kcal/mol and then is only slowly lowered in energy during the remaining generations. The energy of the 26th structure in the population decreases much more slowly, and this is a consequence of the mating and mutation process continuing to form unstable

structures in each generation. After generation 70 only small energy changes occur for lowest and highest energy structures and we take the GA to be converged when the lowest energy structure does not change over the next $3N$ generations, where N is the total number of atoms in the cluster. The average number of generations needed to reach convergence for the $Si_{10}H_m$, $m = 4$, 8, 12, 16, 20, clusters was 83 ± 19, 93 ± 18, 93 ± 9, 136 ± 22, and 155 ± 26, respectively. Since we take the population of a generation as N, the average total number of AM1 geometry optimizations performed was 1162 ± 259, 1680 ± 316, 2039 ± 197, 3527 ± 578, and 4650 ± 769 for $m = 4$, 8, 12, 16, and 20. Thus, with our implementation of the GA, the number of structures evaluated approximately grows only as $\sim O(N^2)$, although this growth still requires the energy evaluation in the GA to be computed rapidly with some simple function such as provided by the AM1 semiempirical method. The present work shows that the semiempirical AM1 method to be useful for ranking energetically the different structures generated by the GA. Unfortunately, the close spacing of the total AM1 energies for different structures requires that B3LYP or MP2 geometry optimizations are also performed to more accurately rank the final structures obtained by the GA. Indeed, one potential drawback to present approach is that the GA searches for the structure with lowest AM1 energy, while the more physically correct structure might have significantly higher AM1 energy and might not be detected when the higher level B3LYP and MP2 calculations are performed. Nonetheless, the GA appears to be doing a good job of providing a relatively small set of low energy candidate structures for further energy analysis by MP2 or B3LYP calculations. Our experience so far suggests this set from the GA contains structures which can give rise to the MP2 or the B3LYP global minimum. Obviously this claim can only be disproved if another optimization method produced even lower energy structures. The inability to directly perform B3LYP or MP2 calculations in the GA is most clearly demonstrated by noting that the actual B3LYP and MP2 calculations on the 10 or 20 lowest AM1 energy structures found by the GA utilized more computer time than all of the AM1 calculations performed in a GA run. Apart from when structures are close in energy, we find the B3LYP and MP2 methods both give very similar cluster geometries and rankings suggesting that we could just use one of the methods for an accurate structure analysis.
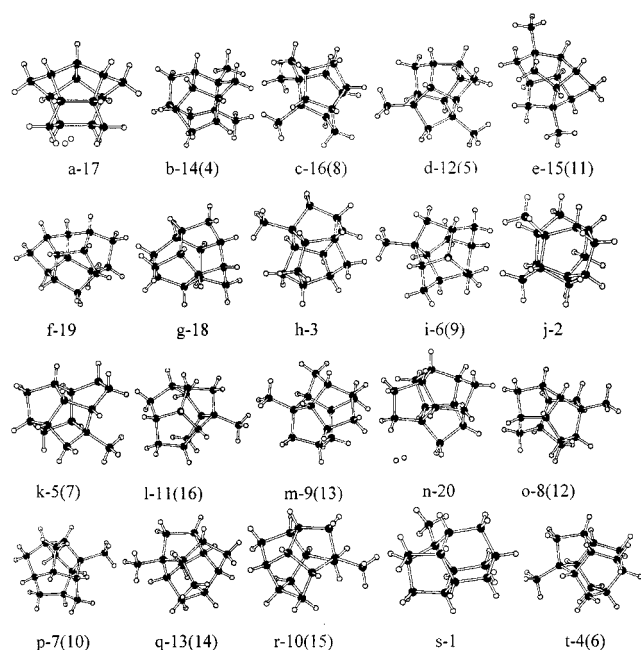
The $\sim O(N^2)$ growth of the number of functions evaluated coupled with the increased computational demands of AM1 calculations on larger clusters requires that other tricks be used in the GA search for the global structure of larger clusters. Below we describe the results of the GA applied to $Si_{14}H_{20}$. The best and safest scheme we have found so far for improved performance is to reduce both the SCF density convergence threshold to 10^{-3} au and gradient convergence threshold to 10^{-3} au in the geometry optimization when generating the initial population of $Si_{14}H_{20}$ structures. We find this significantly shortens the total CPU time without sacrificing the generality and reliability of the GA. The final $Si_{14}H_{20}$ structures described below were produced from 278 generations consisting of 34 structures. We are presently investigating other strategies for more efficient application of the GA to larger passivated Si clusters.

$Si_{14}H_{20}$. An important consideration in the study of nanomaterials is what size particle will cause the bulk like structure and electronic properties to be manifested. Silicon in passivated Si_xH_y clusters can in principle readily form a diamond like lattice. For example, Figure 8 shows the optimized geometry

Global Optimization of Si Clusters

J. Phys. Chem. B, Vol. 106, No. 28, 2002 **7003**
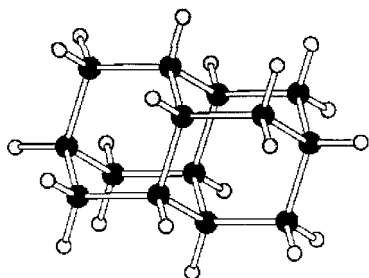
Figure 8. The $Si_{14}H_{20}$ cluster where the Si framework has a diamond lattice-like structure.

a-17   b-14(4)   c-16(8)   d-12(5)   e-15(11)

f-19   g-18   h-3   i-6(9)   j-2

k-5(7)   l-11(16)   m-9(13)   n-20   o-8(12)

p-7(10)   q-13(14)   r-10(15)   s-1   t-4(6)

Figure 9. Twenty lowest AM1 energy structures for $Si_{14}H_{20}$.

obtained at the AM1, MP2 and B3LYP levels for the $Si_{14}H_{20}$ cluster, where the Si atoms were given an initial geometry with a diamond lattice-like arrangement. The average nearest-neighbor Si−Si distance at 2.371 ± 0.009 (AM1), 2.324 ± 0.003 (B3LYP), and 2.312 ± 0.001 Å (MP2) are reasonably close to the experimental 2.3517 Å distance in bulk Si,[36] and all of the Si atoms are tetrahedrally coordinated. However, the final structure obtained in an energy gradient based geometry optimization is dependent on the initial atom coordinates, and the final structure obtained is usually the local minimum closest to the starting geometry. If there was another $Si_{14}H_{20}$ structure at lower energy, a standard gradient based geometry optimization would not find it unless an appropriate starting geometry was given. The GA, on the other hand, does not have a single starting geometry nor is it bound to a particular valley on the potential energy hypersurface. The GA, in principle, should find the structure corresponding to a true global minimum.

Thus as a final test of the GA, using the AM1 energy function, we have attempted to determine whether the diamond like Si structure shown in Figure 8 is the most stable structure for $Si_{14}H_{20}$. We use the refined method outlined in the previous subsection. The resulting 20 lowest AM1 energy structures we obtain for $Si_{14}H_{20}$ from the GA are shown in Figure 9. The GA is clearly successful as it finds 20 structures all with AM1 energies less than that obtained for the diamond structure in Figure 8. Similar to our results for the $Si_{10}H_m$ clusters, we get different AM1, B3LYP, and MP2 energy rankings for the structures. Unfortunately, the Figure 8 diamond like structure

is not among the structures obtained by the GA in Figure 9. The GA structure with the lowest B3LYP and MP2 energies is s-1 and this structure is 5.4 (B3LYP) and 2.6 (MP2) kcal/mol above the diamond like structure in Figure 9. Remarkably structure s-1 is very similar to the diamond structure apart from a five, instead of a six, member Si ring being formed and the addition of SiH_3 to the five-membered ring. Structures j-2 and h-3 exhibit much larger structural differences from the diamond structure but they both differ by less than 0.7 kcal/mol from the s-1 MP2 and B3LYP energies. Thus our calculations show that the GA is not able to guarantee finding the global minimum structure evaluated with a B3LYP or MP2 energy. Nonetheless, it is reassuring that none of the structures in Figure 9 have B3LYP or MP2 energies lower than the corresponding energy found for the diamond structure shown in Figure 8. The GA may in fact be finding the global minimum relative to the AM1 energy, and the reason we are not finding the nonempirical global minimum structure is that we may not be including enough low energy individuals in the GA before satisfying the convergence criterion. Finally, since we are not finding any B3LYP or MP2 energies below the diamond like structure the present results are consistent with the diamond like structure shown in Figure 8 as most likely being the global minimum at the B3LYP and MP2 levels. These relative B3LYP and MP2 energies support the idea that the most stable structure of small H passivated Si clusters is the one where the Si framework adopts a diamond lattice-like structure.

Conclusion

We have developed a genetic algorithm (GA) using optimized AM1 semiempirical energies to find the lowest energy structures of Si_xH_y binary clusters. Coupling the GA with the AM1 energy makes the procedure flexible enough to treat different levels of H passivation for the Si framework in the cluster. The AM1 calculations are inexpensive to perform and, despite being parametrized largely using compounds consisting of four coordinate Si atoms, provide a reasonable starting guess for the partially and fully H-passivated Si clusters. However, quite different energy rankings are obtained with the presumably more physically realistic ab initio calculations. We have found that either B3LYP or MP2 calculations, starting from the optimized AM1 coordinates, can be used to produce very similar structure rankings.

We have applied the GA to the series of clusters $Si_{10}H_m$ with $m = 4$, 8, 12, 16 and 20. With increasing numbers of H atoms the low energy structures evolve from compact Si_{10} cages with some of the Si atoms not fully coordinated to more open structures with all of the Si atoms tetrahedrally coordinated. To accommodate more H atoms when all the Si atoms are four coordinate requires Si ring openings and substantial changes in the Si framework to take place. At the B3LYP and MP2 levels we find the global minimum structure for $Si_{10}H_{16}$ to have a Si framework with a diamond lattice-like structure. We also find evidence that Si_{10} is essentially completely passivated with 16 H atoms, although the GA also indicates that different tetrasilyl cyclopentasilane isomers can be formed by $Si_{10}H_{20}$ at low temperature.

As a further test for how big a Si_xH_y cluster is needed to produce a bulk like Si lattice we also applied a refined GA, with reduced AM1 SCF and optimization tolerances for the initial generation, to the $Si_{14}H_{20}$ cluster. In separate AM1, B3LYP and MP2 calculations we determined the optimized geometry and energy for the $Si_{14}H_{20}$ cluster arranged to have a diamond lattice-like structure. The GA found 20 AM1 structures

all with energies lower than and different from the possible $Si_{14}H_{20}$ diamond lattice-like structure. However, the energies of the B3LYP and MP2 optimized geometries obtained by starting from the AM1 structures were all above the respective B3LYP or MP2 energies computed for the diamond lattice structure. Thus the present calculations are consistent with a relatively small Si_xH_y cluster forming a diamond lattice-like structure as the global minimum at the B3LYP and MP2 energy levels.

References and Notes

(1) Honea, E. C.; Ogura, A.; Murray, C. A.; Raghavachari, K.; Sprenger, W. O.; Jarrold, M. F.; Brown, W. L. *Nature* **1993**, *366*, 42.

(2) Li, S.; Van Zee, R. J.; Weltner, J. W.; Raghavachari, K. *Chem. Phys. Lett.* **1995**, *243*, 275.

(3) Patterson, C. H.; Messmer, R. P. *Phys. Rev. B* **1990**, *42*, 7530.

(4) Rothlisberger, U.; Andreoni, W.; Parrinello, M. *Phys. Rev. Lett.* **1994**, *72*, 665.

(5) Kaxiras, E. *Phys. Rev. B* **1997**, *56*, 13455.

(6) Gong, X. G.; Zheng, Q. Q.; He, Y. *J. Phys.*: *Condens. Matter* **1995**, *7*, 577.

(7) Gong, X. G. *Phys. Rev. B* **1987**, *52*, 14677.

(8) Gingerich, K. A.; Ran, Q.; Schmude Jr., R. W. *Chem. Phys. Lett.* **1996**, *256*, 274.

(9) Jackson, K.; Pederson, M.; Wang, C.; Ho, K. *Phys. Rev. A* **1999**, *59*, 3685.

(10) Sieck, A.; Porezag, Y.; Frauenheim, T.; Pederson, M. R.; Jackson, K. A. *Phys. Rev. A* **1997**, *56*, 4890.

(11) Mitas, L.; Grossman, J. C.; Stich, I.; Tobik, J. *Phys. Rev. Lett.* **2000**, *84*, 1479.

(12) Ho, K. M.; Shvartsburg, A. A.; Pan, B.; Lu, Z. Y.; Wang, C. Z.; Wacker, J. G.; Fye, J. L.; Jarrold, M. F. *Nature* **1998**, *392*, 582.

(13) Katzer, G.; Ernst, M. C.; Sax, A. F.; Kalcher, J. *J. Phys. Chem. A* **1997**, *101*, 3942.

(14) Onida, G.; Andreoni, W. *Chem. Phys. Lett.* **1995**, *243*, 183.

(15) Miyazaki, T.; Uda, T.; Stich, I.; Terakura, K. *Chem. Phys. Lett.* **1996**, *261*, 346.

(16) Meleshko, V.; Morokov, Y.; Schweigert, V. *Chem. Phys. Lett.* **1999**, *300*, 118.

(17) Swihart, M. T.; Girshick, S. L. *Chem. Phys. Lett.* **1999**, *307*, 527.

(18) Niesse, J. A.; Mayne, H. R. *J. Chem. Phys.* **1996**, *105*, 4700.

(19) Luo, Y. H.; Zhao, J.; Qiu, S.; Wang, G. *Phys. Rev. B* **1999**, *59*, 14903.

(20) Iwamatsu, M. J. *Chem. Phys.* **2000**, *112*, 10976.

(21) Rata, I.; Shvartsburg, A. A.; Horoi, M.; Frauenheim, T.; Siu, K. W. M.; Jackson, K. A. *Phys. Rev. Lett.* **2000**, *85*, 546.

(22) Deaven, D. M.; Ho, K. M. *Phys. Rev. Lett.* **1995**, *75*, 288.

(23) Judson, R. S.; Colvin, M. E.; Meza, J. C.; Huffer, A.; Gutierrez, D. *Intl. J. of Quantum Chem.* **1992**, *44*, 277.

(24) Dewar, M. J. S.; Zoebisch, E. G.; Healy, E. F.; Stewart, J. J. P. *J. Am. Chem. Soc.* **1985**, *107*, 3902.

(25) Stewart, J. J. P. *J. Comput. Chem.* **1989**, *10*, 221.

(26) Thiel, W.; Voityuk, A. *J. Mol. Struct.* **1994**, *313*, 141.

(27) Møller, C.; Plesset, M. S. *Phys. Rev.* **1934**, *46*, 618.

(28) Becke, A. D. *J. Chem. Phys.* **1993**, *98*, 5648.

(29) Hay, P. J.; Wadt, W. R. *J. Chem. Phys.* **1985**, *82*, 284.

(30) Rohlfing, C. M.; Raghavachari, K. *Chem. Phys. Lett.* **1990**, *167*, 559.

(31) Dunning, T. H., Jr. Hay, P. J. *Modern Theoretical Chemistry*; Schaefer, H. F., III, Ed.; Plenum: New York, 1977; Vol. 3, p 1.

(32) GAMESS, The General Atomic and Molecular Electronic Structure System. See: Schmidt, M. W.; Baldridge, K. K.; Boatz, J. A.; Elbert, S. T.; Gordon, M. S.; Jensen, J. H.; Koseki, S.; Matsunaga, N.; Nguyen, K. A.; Su, S.; Windus, T. L.; Dupuis, M.; Montgomery, Jr., J. A. *J. Comput. Chem.* **1993**, *14*, 1347.

(33) Frisch, M. J.; Trucks, G. W.; Schlegel, H. B.; Gill, P. M. W.; Johnson, B. G.; Robb, M. A.; Cheeseman, J. R.; Keith, T.; Petersson, G. A.; Montgomery, J. A.; Raghavachari, K.; Al-Laham, M. A.; Zakrzewski, V. G.; Ortiz, J. V.; Foresman, J. B.; Cioslowski, J.; Stefanov, B. B.; Nanayakkara, A.; Challacombe, M.; Peng, C. Y.; Ayala, P. Y.; Chen, W.; Wong, M. W.; Andres, J. L.; Replogle, E. S.; Gomperts, R.; Martin, R. L.; Fox, D. J.; Binkley, J. S.; Defrees, D. J.; Baker, J.; Stewart, J. P.; Head-Gordon, M.; Gonzalez, C.; Pople, J. A. *Gaussian 94*, Revision E.2; Gaussian, Inc.: Pittsburgh, PA, 1995.

(34) Krüger, T.; Sax, A. F. *J. Comput. Chem.* **2001**, *22*, 151.

(35) Dewar, M. J. S.; Jie, C. *Organometallics* **1987**, *6*, 1486.

(36) *CRC Handbook of Chemistry and Physics*, 1st ed.; CRC Press: Boca Raton, FL, 1990.

(37) Scott, A. P.; Radom, L. *J. Phys. Chem.* **1996**, *100*, 16502.